
PROFESSOR GUOHUA XU (Orcid ID : 0000-0002-3283-2392)

DR WEI XUAN (Orcid ID : 0000-0002-4859-2637)

Article type : Original Article

Title: Rice plants respond to ammonium-stress by adopting a helical root growth pattern

Authors:

Letian Jia¹, Yuanming Xie¹, Zhen Wang¹, Long Luo¹, Chi Zhang¹, Pierre-Mathieu Pélissier^{2,3}, Boris Parizot^{2,3}, Weicong Qi⁴, Jing Zhang⁵, Zhubing Hu⁶, Hans Motte^{2,3}, Le Luo¹, Guohua Xu¹, Tom Beckman^{2,3}, Wei Xuan¹[§]

¹State Key Laboratory of Crop Genetics and Germplasm Enhancement and MOA Key Laboratory of Plant Nutrition and Fertilization in Lower-Middle Reaches of the Yangtze River, Nanjing Agricultural University, Nanjing 210095, PR China

²Department of Plant Biotechnology and Bioinformatics, Ghent University, Technologiepark 71, B-9052 Ghent, Belgium

³VIB-UGent Center for Plant Systems Biology, Technologiepark 71, B-9052 Ghent, Belgium

⁴Institute of Agricultural Resources and Environment, Jiangsu Academy of Agricultural Sciences, Nanjing 210014, China

⁵State Key Laboratory of Plant Physiology and Biochemistry, College of Biological Sciences, China Agricultural University, Beijing 100193, China

⁶Key Laboratory of Plant Stress Biology, School of Life Sciences, Henan University, Kaifeng 475004, China

This article has been accepted for publication and undergone full peer review but has not been through the copyediting, typesetting, pagination and proofreading process, which may lead to differences between this version and the [Version of Record](#). Please cite this article as [doi: 10.1111/TPJ.14978](https://doi.org/10.1111/TPJ.14978)

This article is protected by copyright. All rights reserved

[§]Corresponding author: wexua@njau.edu.cn

Running title: Ammonium triggers a helical response of rice root

Accepted Article

Abstract:

High levels of ammonium nutrition reduce plant growth and different plant species have developed distinct strategies to maximize ammonium acquisition while alleviate ammonium toxicity through modulating root growth. Up to now, the mechanism underlying plant tolerance or sensitivity towards ammonium remain unclear. Rice uses ammonium as its main N source. Here we show that ammonium supply restricts rice root elongation and induces a helical growth pattern, which is attributed to root acidification resulting from ammonium uptake. Ammonium-induced low pH triggers asymmetric auxin distribution in rice root tips through changes in auxin signaling, thereby inducing a helical growth response. Blocking auxin signaling completely inhibited this root response. In contrast, this root response is not activated in ammonium-treated *Arabidopsis*. Acidification of *Arabidopsis* roots leads to the protonation of IAA, and dampening the intracellular auxin signaling levels that are required for maintaining root growth. Our study suggests a different mode of action by ammonium on the root pattern and auxin response machinery in rice versus *Arabidopsis*, and the rice-specific helical root response towards ammonium is an expression of the ability of rice in moderating auxin signaling and root growth to utilize ammonium while confronting acidic stress.

Key word:

Ammonium, helical root response, root elongation, auxin, acidic stress, *Oryza.sativa L.*, *Arabidopsis thaliana*

Introduction

Nutrient availability is known to impact plant development and physiology, and activate root foraging responses, including physiological and developmental changes of the root. Nitrogen (N) is one of the most essential nutrients for plants, and its availability largely affects plant root elongation and branching. Previous studies in the model plant *Arabidopsis thaliana* have revealed distinguished root behaviors to different nitrogen forms. As its preferred N form, nitrate (NO_3^-) stimulates root elongation and lateral root branching, while ammonium (NH_4^+) exhibits toxicity on *Arabidopsis* root development and suppresses root elongation (Giehl and von Wiren 2014, Li *et al.* 2014a).

In *Arabidopsis*, the NO_3^- -regulated root response has been intensively studied and suggested to be governed by a molecular regulatory network constituted of nitrate transporters, transcription factors, and protein kinases (Gaudinier *et al.* 2018, Liu *et al.* 2017, O'Brien *et al.* 2016). Plant hormones, e.g. auxin (Krouk *et al.* 2010, Wang *et al.* 2019), cytokinins (Poitout *et al.* 2018), brassinosteroids (Jia *et al.* 2019), and signaling peptides (Araya *et al.* 2014, Ohkubo *et al.* 2017, Tabata *et al.* 2014), have also been found to mediate NO_3^- -dependent root responses through their signaling and transport pathways. In contrast, only few signaling molecules, e.g. AMT/MEP/Rh-type ammonium transporters (AMTs) (Lima *et al.* 2010), and its regulator CIPK23 (Straub *et al.* 2017), have been so far identified to regulate root responses to NH_4^+ in *Arabidopsis*, while the regulatory mechanism of these molecular components during this process is not well understood (Xuan *et al.* 2017).

Unlike *Arabidopsis*, NH_4^+ is the preferred N form for crop rice (*Oryza sativa L.*) in the paddy field. High NH_4^+ supply has previously been found to reduce rice seminal root (SR) elongation (Hirano *et al.* 2008, Xuan *et al.* 2013), though the underlying mechanism remains elusive. Meanwhile, a detailed analysis of root responses to N regimes in rice is still lacking and it is also unclear whether rice roots respond to N regimes in a similar pattern/mechanism as *Arabidopsis*. Noticeably, in a recent study, brassinosteroid biosynthesis has been shown to involve in NH_4^+ -inhibited rice root elongation, proposing a potential role of plant hormones in regulating rice root response to N (Jiao *et al.* 2019). Common to all plants, plant hormone auxin plays a critical

role in regulating rice root development (Meng *et al.* 2019), and its signaling is also moderated under high NH_4^+ (Di *et al.* 2018), implying that auxin might also be implicated in N-triggered root responses in rice.

To address these issues, in this study, we performed detailed analysis on the root responses of rice and *Arabidopsis* to high NH_4^+ . We show that high levels of ammonium rather than nitrate suppress the rice root elongation, and interestingly, trigger a helical root response, which is induced by the acidic stress as a result of ammonium uptake by root. We demonstrate that activation of helical root response by ammonium and low pH is mediated by auxin signaling and can be suppressed when auxin signaling is blocked. However, this root response is not observed in NH_4^+ -treated *Arabidopsis*, due to the inactivation of cellular auxin signaling. Furthermore, we showed that this helical root response is reversible and temporally activated when root is subjected to acidic stress. Our results thereby reveal a root response adopted by rice plants to confront acidic stress during its root foraging for N sources.

Results

NH_4^+ treatment induces a helical root response in rice

We first studied the root response to nitrogen regimes in rice by using a hydroponic system. Rice cultivar Nipponbare (NIP) seedlings were grown in hydroponic solutions supplied with different nitrogen forms, including ammonium (NH_4^+), nitrate (NO_3^-), and their combination (NH_4NO_3), whereas a solution without nitrogen (N-free, -N) was used as a control. NH_4^+ and NO_3^- were both supplied at 2.5 mM, a concentration promoting rice shoot growth (Figure S1a,b) (Luo *et al.* 2018, Wang *et al.* 2018). In terms of root development, different donors of NH_4^+ (NH_4Cl and $(\text{NH}_4)_2\text{SO}_4$), as well as the combination of NH_4^+ and NO_3^- (NH_4NO_3), caused a significant and identical reduction on SR elongation of rice seedlings as compared to the N-free treatment (-N), whereas NO_3^- treatment alone (KNO_3) did not affect the SR elongation (Figure 1a,b). The NH_4^+ -inhibited seminal root elongation is probably resulted from the decreased cell division activity in root meristem because a shorter root meristem with less cortical cells was observed under ammonium treatment compared to N-free treatment (Figure S2). Interestingly, in the

medium supplied with NH_4^+ , SRs were observed to spiral at their tips, thus exhibiting a helical growth pattern, which was not observed neither in N-free nor NO_3^- treated SRs (Figure 1a,b). This helical growth response depended on the concentration of NH_4^+ with a monitoring checkpoint at 0.5 mM (Figure S1c-e). The same skewing response could also be observed in the root tips of seedlings grown inside the agar media supplied with high NH_4^+ (Figure S3). Furthermore, at later development stages of rice seedlings, the adventitious root tips rather than lateral roots were also found to spiral upon high NH_4^+ (Figure S4). These data strongly suggest that the root helical growth response is a general response of the rice seminal and adventitious roots to ammonium.

However, it is unclear whether NH_4^+ -triggered root spiraling is due to the loss of root sensitivity to gravity. To address this, we performed time-lapse imaging following the root tip growth in the hydroponic system over 48 hours. Upon N deprivation, the rice root tips circumnated and grew downward in response to gravity, whereas in the medium supplied with NH_4^+ , the root tips completely changed their growth direction and started to spiral after 36-h treatment (Figure 1c, and Movie S1), demonstrating that this root response is resulting from the loss of root gravitropism.

Helical root response is caused by the root acidification resulted from root NH_4^+ uptake

As this root helical growth response is triggered by NH_4^+ treatment, we questioned whether or not it is caused by NH_4^+ uptake. In plants, NH_4^+ uptake is governed by ammonium transporters (AMTs) (Loque and von Wiren 2004, Xuan, Beekman and Xu 2017), we therefore analyzed the root phenotypes of rice *OsAMT1.1* knock-out lines (*Osamt1;1-1* and *Osamt1;1-2*) and an over-expression line (*pUBIL:OsAMT1;1*). Under N-free and NH_4^+ treatments, the root of *Osamt1;1* knock-out mutant behaved the same as WT (Figure S5a,b), which might be due the redundancy of different OsAMTs in uptake of NH_4^+ . In contrast, the *OsAMT1.1* over-expression line was hyper-sensitive to NH_4^+ treatment: a faster helical growth response and shorter SR were observed in the over-expression line compared to WT after 24-h treatment (Figures 1d,e, and S5c). These data indicate the importance of NH_4^+ -uptake on root elongation and helical growth, which could be enhanced when root NH_4^+ uptake is increased.

Previous studies have shown that NH_4^+ uptake by plant roots is synchronized with a pronounced proton release from the root surface, resulting in external acidification (Ortiz-Ramirez *et al.* 2011, Zhu *et al.* 2009). Transcriptional analysis of ammonium transporter *OsAMT1;1* by using transgenic *pOsAMT1;1:nls-GUS* reporter line showed a strong expression of *OsAMT1;1* at root tip and emerged lateral roots. Remarkably, *OsAMT1;1* strongly expressed at the outer layer tissues of the distal root meristem zone, with a relative weak expression at elongation zone and differentiation zone (Figure S6). Consistently, by measuring the changes of NH_4^+ and protons in the microenvironment surrounding the root, we detected a fast uptake of NH_4^+ by the root tip upon NH_4^+ treatment, followed by a pronounced proton release (Figure 2a). Further long-term measurements of pH in the NH_4^+ -supplied medium and visualization of color-changing medium containing the bromocresol purple (BCP) pH indicator (Gujas *et al.* 2012), both displayed a significant reduction of pH in NH_4^+ supplied medium within 24 hours, while the pH in the NO_3^- -supplied medium was slightly increased (Figure S7, and Movie S2). These data suggest that proton release during the NH_4^+ uptake leads to acidification of the root environment. Notably, specifically in the root tip region, comprising the meristem and elongation zone (0 ~ 600 μm from the tip), we detected a strong proton influx into the root tip region upon NH_4^+ treatment (Figure 2a), which might directly acidify the local root cells. Indeed, by staining the root tip segments of NH_4^+ -treated seedlings with the pH indicator BCP, we observed an obvious color change of the solution to yellow (Figure 2b), confirming the acidification of the root tissues. In plants, the proton flux in roots is facilitated by plasma membrane (PM) PM- H^+ -ATPases (Yan *et al.* 1998). Addition of the ATPase inhibitor N,N'-dicyclohexylcarbodiimide (DCCD) attenuates the acidification of the medium and restored the root sensitivity to gravity and SR elongation under NH_4^+ treatment (Figures 2c-e, and S8). Altogether, our results strongly suggest that NH_4^+ uptake facilitates proton exchange between roots and their environment, and may result in acidic stress to the rice roots.

Acidic stress has been shown to negatively regulate the elongation of plant roots by repressing meristem cell division and elongation (Gujas, Alonso-Blanco and Hardtke 2012, Pacheco-Villalobos *et al.* 2016). We thus investigated whether rice root gravitropism and elongation could be altered under acidic conditions by growing rice WT seedlings in low pH

medium. Remarkably, the root helical growth response, as well as a substantial reduction on SR elongation, was also observed in the medium with low pH (≤ 4.5 , adjusted with MES), regardless of NH_4^+ supplies (Figure S9a,b). When the medium pH was adjusted to 2.5, the SR elongation was severely inhibited while the root tip displayed a U-turn (Figure S9a,b). Moreover, quantification of the proton flux by the root under low pH conditions showed a similar strong proton flux into the root tip region comprising the meristem and elongation zone (Figure S9c), resembling the proton influx dynamic under high NH_4^+ condition. These results reveal a similar effect of NH_4^+ and acidic stress on root acidification and root responses, and thus raise the possibility that NH_4^+ -mediated root responses could be attributed to acidic stress resulting from NH_4^+ uptake.

To verify our hypothesis, the buffer agent 2-Morpholinoethanesulfonic acid monohydrate (MES) was added into the medium to reduce proton fluctuation in the medium. Intriguingly, addition of 2.5 mM or higher concentrations of MES to the NH_4^+ supplied medium suppressed the NH_4^+ -triggered medium acidification, proton exchanges in the root tip, and root acidification (Figures 2a, 3a, S10a,b, and Movie S3). Accordingly, the NH_4^+ -dependent inhibition of root meristem activity, root elongation and sensitivity to gravity were both recovered by MES (Figures 3b,c, S10c,d, and Movie S1). Collectively, these data demonstrate that this tropic root response might be transiently activated when roots suffer from acidic stress.

NH_4^+ -induced helical response of rice root is mediated by auxin signaling

Plant root gravitropism is facilitated by auxin redistribution in the lateral root cap and epidermis at the root tip (Band *et al.* 2012, Swarup *et al.* 2005). To inspect the correlation of the helical growth response with auxin redistribution, the expression pattern of auxin responsive reporter *DR5rev:3xVENUS-N7* in rice root apices was analyzed, and an asymmetric distribution of *DR5* expression in the lateral root cap and epidermis was induced in root tips of rice seedlings by both NH_4^+ treatment (- MES) and low pH, which is in concert with the observation of helical root responses under these conditions (Figure 4a-c). This asymmetric *DR5* distribution in the root tip was eliminated when NH_4^+ -induced acidification was prevented by the supply of MES in the culture medium (Figure 4a-c). It thus confirms the involvement of auxin redistribution in the root

helical response triggered by NH_4^+ -induced acidification.

The asymmetric distribution of auxin in the root tip has been implicated to be controlled by its biosynthesis, transport, and signaling pathways (Adamowski and Friml 2015, Band, Wells, Larrieu, Sun, Middleton, French, Brunoud, Sato, Wilson, Peret, Oliva, Swarup, Sairanen, Parry, Ljung, Beeckman, Garibaldi, Estelle, Owen, Vissenberg, Hodgman, Pridmore, King, Vernoux and Bennett 2012, Baster *et al.* 2013, Zhang *et al.* 2019a, Zhang *et al.* 2019b). We therefore next validated the role of auxin in the helical growth response by using diverse functional unrelated auxin pathways inhibitors, including the auxin efflux carrier inhibitors NPA and BUM (Henrichs *et al.* 2012, Kim *et al.* 2010, Teale and Palme 2018), the auxin influx carrier inhibitor 1-NOA (Parry *et al.* 2001), the YUC-mediated auxin biosynthesis inhibitor YUCCASIN (Nishimura *et al.* 2014), and the auxin receptor inhibitor PEO-IAA (Hayashi *et al.* 2012). Application of NPA, BUM, and 1-NOA only suppressed the NH_4^+ -induced helical growth response, whereas PEO-IAA and YUCCASIN restored both the root gravity and elongation (Figures 4d-f, and S11).

Intriguingly, the NH_4^+ -induced acidification was not alleviated by any of the used chemicals (Figure 4g, h), indicating that auxin acts downstream of NH_4^+ uptake to mediate helical root growth. Altogether, our data demonstrate a critical role of auxin transport and signaling in mediating NH_4^+ -triggered root responses.

Ammonium uptake also causes root acidification, but only represses root elongation without inducing helical root growth in Arabidopsis

To test whether the inhibition of NH_4^+ on root elongation and gravitropism is a general phenomenon for plants, we further investigated the root phenotype in the model plant Arabidopsis. High NH_4^+ has been reported to negatively regulate Arabidopsis root growth (Cao *et al.* 1993, Li *et al.* 2014b, Zou *et al.* 2012). However, these studies were conducted with growth media supplemented with MES, attenuating the proton fluctuation. To inspect whether NH_4^+ responses are pH-dependent in Arabidopsis, the root phenotype upon varying concentrations of NH_4^+ and NO_3^- was first analyzed in MES-free medium. Similar to the rice root, the Arabidopsis PR was strongly acidified and shorter upon high NH_4^+ treatment as compared to roots under N-free

conditions, while NO_3^- treatment alkalized the root and stimulated the PR elongation (Figure S12); the activity of root meristem is also reduced by NH_4^+ treatment (Figure S14). The inhibition of NH_4^+ on root elongation and meristem activity could be fully recovered when the medium pH was buffered with MES (Figures 5a,b, S13a,b, and S14); low pH treatment also substantially reduced the PR elongation (Figure S13c,d). In addition, both high NH_4^+ and low pH treatments were found to stimulate a transient proton influx to the root meristem and elongation zone (Figure 5d,e). These data strongly suggest that NH_4^+ inhibited Arabidopsis root elongation by inducing acidic stress in cells of the root meristem and elongation zone.

We further confirmed that NH_4^+ triggered root acidification and root responses also resulted from the NH_4^+ uptake. In the quadruple ammonium transporter (*amt1;1amt1;2amt1;3amt2;1* mutant) *qko* mutant of *AtAMTs*, which reduces root NH_4^+ uptake (Lima, Kojima, Takahashi and von Wiren 2010, Straub, Ludewig and Neuhauser 2017), high NH_4^+ -inhibited PR elongation was relieved in the absence of MES, and was accompanied by reduced influx of NH_4^+ and proton to the root meristem (Figure 5a,b,d). Nevertheless, the root development of the *qko* mutant remained sensitive to acidic stress as low pH treatment strongly reduced PR elongation of *qko* mutant and induced strong proton influx to the root, to the same extent of Col-0 seedlings (Figure 5a,b,e). These results further implicate that the PR tolerance of *qko* to NH_4^+ is due to the reduced NH_4^+ uptake by root.

We noticed that the Arabidopsis root did not exhibit a helical growth upon high NH_4^+ treatment (Figure 5a,c), and quantification of *DR5rev:3xVENUS-N7* signal showed a symmetric distribution of DR5 expression in the lateral root cap (LRC) and epidermis under high NH_4^+ (Figure S15a,b). Interestingly, DR5 signal was substantially reduced in the vascular tissue of the roots upon either low pH or NH_4^+ treatment, and NH_4^+ -repressed DR5 expression in stele can be fully recovered by supplying MES (Figure S15a,b). Using another auxin sensitive sensor DII-VENUS, which is rapidly degraded in the presence of auxin (Brunoud *et al.* 2012), we observed enhanced nuclear DII signal in the root meristem under high NH_4^+ (-MES) and low pH treatments (Figure 5f,g). Thus, the reduced PR elongation might be caused by the decrease of cellular auxin signaling in the root meristem under acidic stress.

The cellular auxin signaling in roots relies on its receptor TIR1 and a sufficient level of auxin, which is modulated by auxin transporters. To our surprise, auxin signaling mutants (*tir1afb2*, *slr-1*, and *arf7arf19*), as well as auxin transport mutants (*aux1-21*, *pin2*, *pid*, and *d6pk013*) remained sensitive to NH_4^+ or low pH treatment towards PR elongation (Figure S15c,d). Similarly, the typical agravitropic root response of the *aux1* mutant, with a defective auxin influx carrier, was not affected (Figure S15c,d). It therefore seems that auxin signaling and transport are not accounted for NH_4^+ -inhibited Arabidopsis root elongation.

Under acidic environment, IAA is protonated into IAAH. Whereas IAA uptake requires the plasma membrane-localized AUX1 auxin influx carrier (Swarup and Peret 2012), IAAH is able to cross the cell membrane via diffusion (Delbarre *et al.* 1996, Gutknecht and Walter 1980). Similar as in the WT, NH_4^+ or low pH treatment inhibited the PR elongation in the *aux1-21* mutant (Figure S15c,d). Quantification of the DII signal in the *aux1-21* mutant showed that NH_4^+ and low pH did not affect the nuclear DII signal in the LRC and epidermis, but still enhanced the nuclear DII signal in the root vascular tissue of the *aux1-21* mutant (Figure 5f,g). Thus, the reduced auxin signaling in the vascular tissue does not require AUX1 function, but might depend on IAAH diffusion.

To assess this possibility, exogenous IAA, NPA, and synthetic IAA analogue 1-naphthalene acetic acid (1-NAA) were supplied to NH_4^+ - or low pH-treated Arabidopsis roots. Unlike IAA, 1-NAA readily permeates the cell membrane independent of auxin transporters (Dindas *et al.* 2020). We found that NAA treatment could trigger the degradation of nuclear DII signal at the vascular tissues in the root meristem regardless of NH_4^+ supply or low pH, while NH_4^+ supply (-MES) or low pH upon IAA treatment sustained DII signal in the presence of IAA (Figure S16). The auxin efflux carrier inhibitor NPA led to IAA accumulation in root cells and eliminated the DII signal under NH_4^+ (+ MES), but the NPA-induced DII degradation could be significantly suppressed under NH_4^+ (-MES) or low pH treatments (Figure S16), implicating that the reduced cellular auxin signaling level is independent of active auxin transport. These data strongly suggest that the reduced auxin signaling under NH_4^+ and low pH might be a result of increased diffusion of auxin due to its protonation.

The helical root response is critical for root tolerance to NH_4^+ uptake-induced acidic stress

Our above results strongly suggest distinct regulations of NH_4^+ nutrition on the root growth response and auxin signaling between rice and Arabidopsis, raising the question whether the helical root response is accounted for rice tolerance to high ammonium nutrition. Interestingly, when high NH_4^+ - or low pH-pretreated rice seedlings, which show helical and shorter SR roots, were transferred from MES-free medium to MES-supplied medium with pH at 5.5, both the SR elongation and root gravitropic response were fully restored (Figure 6a,b). On the contrary, NH_4^+ -inhibited Arabidopsis root elongation was only partially restored when the seedlings were transferred to MES-supplied medium, while low pH (4.5)-inhibited root growth cannot be rescued when the seedlings were transferred to medium with pH adjusted to 5.8 (Figure 6c,d). These results indicate that compared to Arabidopsis, rice has the capacity to perceive rapid changes of environmental pH and can activate a helical root response that allows a more efficient recovery beyond the NH_4^+ stress, which might represent a strategy of rice plants to alleviate high ammonium and acidic stresses.

Discussion

In summary, our results demonstrate that the NH_4^+ -inhibited root development in both rice and Arabidopsis is attributed to the root acidification as a result of proton release during NH_4^+ uptake by root. Acidic stress has been reported to inhibit root elongation by restricting root meristem activity in plants (Gujas, Alonso-Blanco and Hardtke 2012, Pacheco-Villalobos *et al.* 2016). Our results reveal that high NH_4^+ and low pH trigger a strong proton influx into the root meristem and elongation zone thus causing acidic stress and repressing root elongation.

Plants can adapt their root growth (i.e. growth direction) in relation to environmental stimuli through modulating auxin signaling (Feng *et al.* 2016, Korver *et al.* 2018, Orman-Ligeza *et al.* 2018). In this study, we discover a helical root growth response under high NH_4^+ supply and acidic stress in rice. Remarkably, NH_4^+ - and low pH-induced helical root response is reversible and root elongation can be fully restored when the rice plants are no longer suffered from acidic stress

(Figure 6). It further indicate that this typical root response is temporally activated for rice plant to alleviate the acidic stress resulted from its ammonium uptake.

We further demonstrated that this typical response of rice roots to NH_4^+ and acidic stress is due to the loss of root gravity whereas an asymmetric distribution of auxin was induced in the LRC and epidermal cells at the root tip (Figure 4), indicative of elevated sensitivity of rice roots to pH changes. Application of auxin biosynthesis, signaling and transport inhibitors all suppressed the NH_4^+ and low pH-induced asymmetric DR5 distribution and root spiraling (Figure 4d-f), suggesting the involvement of auxin biosynthesis, signaling and transport in mediating this rice root helical root response to ammonium and low pH in rice.

However, auxin transporter inhibitors and auxin biosynthesis and signaling inhibitors exhibited divergent effects in rescuing NH_4^+ and low pH-inhibited root elongation. Auxin transport inhibitors (NPA, BUM and 1-NOA) were found to restrain root elongation at either N-free or NH_4^+ and low pH conditions (Figure S11). The overall inhibition on root elongation by auxin transport inhibitors under different treatments indicates that auxin transport is essential for maintaining root elongation, but is not specifically for root acidification caused by NH_4^+ uptake. In contrast, application of auxin biosynthesis and signaling inhibitors, Yucasin (YUC inhibitor) and PEO-IAA (TIR1 inhibitor), significantly rescued the root elongation under either NH_4^+ or low pH treatment, without affecting root elongation at N-free condition (Figures 4d-f, and S9). Thus, NH_4^+ and root acidification caused inhibition on root elongation might act specifically through auxin biosynthesis and signaling pathways. Recent studies have linked auxin and its signaling pathway to the pH-dependent cell elongation in plants (Barbez *et al.* 2017, Dang *et al.* 2020, Fendrych *et al.* 2016). Our results highlighted a critical role of auxin biosynthesis content and signaling on mediating NH_4^+ and low pH-triggered root elongation in rice plants.

On the other side, NH_4^+ and low pH treatments both inhibited meristem activity and elongation of Arabidopsis root, but did not alter the root gravitropic response (Figures 5a,b, S12 and S13). Our results further showed that the regulation of NH_4^+ and low pH on Arabidopsis root development overrides the canonical auxin signaling pathway and auxin transport, mainly through the moderation of the chemical form of auxin (Figures 5f,g, S15 and S16). These results reveal

different regulatory mechanisms on auxin signaling between rice and Arabidopsis roots regarding acidic stress, and rice might develop an uncharacterized signaling pathway to activate auxin signaling to moderate its root growth regarding NH_4^+ and low pH.

In contrast to plants growing in well-aerated soils (e.g. Arabidopsis), rice uses NH_4^+ as its main inorganic nitrogen in paddy field conditions and might have developed a strategy to adjust root growth in order to optimize access to NH_4^+ and to cope with NH_4^+ uptake-induced acidic stress. This is highlighted by the recovery experiment: the inhibited root growth and gravitropic response by NH_4^+ and acidic stresses could be fully recovered when the roots were transferred to normal condition, whilst Arabidopsis root is largely restrained and gradually ceases, and root growth could not be alleviated after transfer. The difference of root tolerance to NH_4^+ and acidic stresses between rice and Arabidopsis might be attributed to their distinguished regulatory mechanisms on auxin signaling. The capacity to manipulating auxin signaling pathways under high ammonium and acidic stresses confers the rice root tolerance to these stresses. However, the signaling molecule that transmits the external or internal NH_4^+ uptake-induced acidic status to auxin signaling for helical root response remain uncharacterized in rice, and will be further investigated.

In summary, our discovery of helical root response in rice regarding ammonium highlights its ability on controlling root pattern to utilize ammonium and avoid acidic stress in paddy field, and pave ways to enhance plant tolerance to ammonium and acidic stresses through moderating auxin signaling pathways.

EXPERIMENTAL PROCEDURES

Plant materials

Wild-type lines of rice (*Oryza sativa*.L, cultivars Nipponbare and 9322) and *Arabidopsis thaliana* Col-0 were used in this study. The rice homozygous *UBIL:AMT1;1* overexpression line and *OsAMT1.1* knock-out mutants are Nipponbare background and were generated in a previous study (Li *et al.* 2016). Rice *DR5rev:3xVENUS-N7* transgenic reporter line is in Wuyunjing-7 (9322) background and described previously (Yang *et al.* 2017).

Arabidopsis transgenic reporter lines and mutants have been earlier described: *DII-VENUS* (Brunoud, Wells, Oliva, Larrieu, Mirabet, Burrow, Beeckman, Kepinski, Traas, Bennett and Vernoux 2012), *DR5rev:3xVENUS-N7* (Xuan *et al.* 2016), *qko* mutant of *AtAMTs* (Lima, Kojima, Takahashi and von Wiren 2010), *arf7arf19* (Okushima *et al.* 2005), *tir1afb2* (Parry *et al.* 2009), *slr-1* (Fukaki *et al.* 2002), *d6pk013* (Zourelidou *et al.* 2009), *aux1-21* (Swarup *et al.* 2004), and *pin2* (Muller *et al.* 1998).

Plant growth conditions

Rice and *Arabidopsis* seeds of wild-type, transgenic and mutant lines were sterilized with 70% (v/v) ethanol for 1 min, followed by 30% (v/v) sodium hypochlorite solution for 30 min (rice) or 15 min (*Arabidopsis*). *Arabidopsis* seeds were then kept at 4 °C in the refrigerator for 3 days imbibition, whereas rice seeds were germinated in water and in the dark at 37 °C for 3 days.

Geminated rice seedlings were first grown in water for 3 days in a growth chamber under a photoperiod of 14 h light ($\sim 200 \mu\text{mol m}^{-2} \text{s}^{-2}$ light density and $\sim 70\%$ humidity) and a temperature of 28 °C, and rice seedlings with 2 cm long SR were then transferred to the hydroponic culture supplied with modified Kimura B solution (500 mL volume for each cup with 10 seedlings) for different N treatments. The modified Kimura B solution (pH 5.5, adjusted with KOH) contained 1.25 mM $(\text{NH}_4)_2\text{SO}_4$, 2.5 mM KNO_3 , 1 mM CaCl_2 , 0.3 mM KH_2PO_4 , 0.35 mM K_2SO_4 , 1 mM $\text{MgSO}_4 \cdot 7\text{H}_2\text{O}$, 0.5 mM $\text{Na}_2\text{SiO}_3 \cdot 5\text{H}_2\text{O}$, (0.54), 9 μM $\text{MnCl}_2 \cdot 4\text{H}_2\text{O}$, 0.39 μM $\text{Na}_2\text{MoO}_4 \cdot 2\text{H}_2\text{O}$, 20 μM H_3BO_3 , 0.77 μM $\text{ZnSO}_4 \cdot 7\text{H}_2\text{O}$, 0.32 μM $\text{CuSO}_4 \cdot 5\text{H}_2\text{O}$ (0.32), and 20 μM Fe(II)-EDTA. For N-free treatment, nitrogen sources $(\text{NH}_4)_2\text{SO}_4$ and KNO_3 was replaced with K_2SO_4 at a

concentration of 1.25 mM; for NH_4^+ treatment alone, KNO_3 was replaced with K_2SO_4 at the same concentration. The 2-[morpholino]ethanesulfonic acid (MES) was supplied to hydroponic cultures to buffer pH of the medium when mentioned. The rice seedlings were treated for 4 days unless otherwise noted and the nutrient solution was renewed every two days.

Arabidopsis seeds were sown in the transparent Petri dishes (12 cm X 12 cm) supplied with sterile modified MS medium (1 % [w/v] Sucrose, 0.8 % [w/v] agar, and 0.5 g/L MES, pH 5.8, adjusted with KOH), and grown vertically under continuous light conditions ($100 \mu\text{mol m}^{-2} \text{s}^{-1}$) and at a temperature of 21 °C. The modified MS medium contained 10 mM $(\text{NH}_4)\text{SO}_4$, 19.5 mM KNO_3 , 1 mM KH_2PO_4 , 3 mM $\text{CaCl}_2 \cdot 2\text{H}_2\text{O}$, 15 mM $\text{MgSO}_4 \cdot 7\text{H}_2\text{O}$, 5 μM KI, 0.1 mM H_3BO_3 , 0.1 mM $\text{MnSO}_4 \cdot \text{H}_2\text{O}$, 30 μM $\text{ZnSO}_4 \cdot 7\text{H}_2\text{O}$, 1 μM $\text{Na}_2\text{MoO}_4 \cdot 2\text{H}_2\text{O}$, 0.1 μM $\text{CuSO}_4 \cdot 5\text{H}_2\text{O}$, 0.1 μM $\text{CoCl}_2 \cdot 6\text{H}_2\text{O}$, 0.1 mM $\text{FeSO}_4 \cdot 7\text{H}_2\text{O}$, 0.1 mM $\text{Na}_2\text{EDTA} \cdot 2\text{H}_2\text{O}$, and 0.1 g/L myo-inositol.

For NH_4^+ treatment alone, KNO_3 was replaced with KCl at the same concentration, 2.5 mM $(\text{NH}_4)\text{SO}_4$ was used as NH_4^+ donor except as otherwise indicated ; For N-free conditions, nitrogen sources $(\text{NH}_4)_2\text{SO}_4$ and KNO_3 was replaced with KCl at a concentration of 10 mM. To access the effect of pH on root development, MES was removed from the medium in some experiments as mentioned.

Chemical preparation and treatments

N,N'-dicyclohexylcarbodiimide (DCCD), 1-N-naphthylphthalamic acid (NPA), 1-Naphthylacetic acid (NAA), and 5-(4-chlorophenyl)-4H-1,2,4-triazole-3-thiol (YUCASIN) were ordered from Sigma-Aldrich. 2-[4-(diethylamino)-2-hydroxybenzoyl]benzoic acid (BUM) and PEO-IAA were described previously (Hayashi, Neve, Hirose, Kuboki, Shimada, Kepinski and Nozaki 2012, Kim, Henrichs, Bailly, Vincenzetti, Sovero, Mancuso, Pollmann, Kim, Geisler and Nam 2010). All chemicals were dissolved in 100% dimethylsulfoxide (DMSO) to make a 50 mM stock solution.

The working concentrations of the chemicals are indicated in the respective figure legends. For chemical treatments on Arabidopsis in agar plates, the required amount of the stock solutions of the chemicals was first supplied to 50 mL falcon tubes containing 1/2 MS agar medium and mixed before being poured into Petri dishes. For chemical treatments on rice seedlings in

hydroponic solution, chemicals were added into the liquid Kimura B solution and mixed before the seedlings were transferred.

Quantitative analysis of root elongation

To record the root phenotypes, rice and Arabidopsis seedlings were scanned at 600 dpi by using Epson scanner Expression 11000XL after treatment, and root growth parameters (seminal/primary root elongation and helical index) were analyzed using Fiji image analysis software (<http://fiji.sc/>). However, different strategies were applied to quantify the root phenotypes of Arabidopsis and rice.

To quantify the elongation of rice seminal root (SR), germinated rice seedlings with ~ 2 cm long SR were selected and scanned before and after treatments, and the length of newly formed SR region during the treatments was calculated as SR length. On the other hand, the Arabidopsis root elongation was also quantified by measuring the length of the newly formed primary root region after transfer.

Quantification of root helical index

The helical root response is only observed at the root tip, and the helical index of rice roots is obtained by calculating the ratio of helical distance and linear distance in the root tip region. To clarify, the linear distance is the seminal root length between the root tip to a certain point at the root that is apart from the root tip. For all the roots used for measurements in this study, the linear distance is fixed to 2 cm, and the point at the root which is 2 cm from the root tip is marked for subsequent measurement of helical distance. The helical distance is the straight-line distance between the root tip and the marked point at the root. The helical distance and linear distance were measured with Fiji image analysis software. In addition, The angle of rice and Arabidopsis root tip from the vertical plane was also recorded by using the same software after imaging.

Medium pH measurement and bromocresol purple staining

To detect medium pH acidification by rice seedling roots, 10 seedlings were incubated in the

hydroponic culture (500 mL volume) for 2 days, and the pH of the medium was recorded every 24 hours by using a Sartorius PB-10 pH meter (Sartorius, Germany).

To visualize pH changes of the media over time, the rice seedlings were transferred into the transparent plastic pots containing different media, in which the pH-sensitive indicator bromocresol purple (BCP), with a sensitivity range of pH 5.2–6.8, was added to reach a final concentration (0.006% (w/v)). The images were taken every 5 min over 48 hours to record the changes of medium color indicated by BCP.

To check the root acidification, the root tips (2~3 cm) collected from 5 rice or 10 Arabidopsis seedlings were harvested from different treatments and immediately transferred to 1.5 ml Eppendorf tube containing 1 mL 0.006% (w/v) BCP. After 15 min incubation at room temperature, the Eppendorf tubes were imaged.

Measurements of net proton and NH₄⁺ flux

A BIO-IM Series NMT Physiolyzer® system (YoungerUSA) was applied to determine the net proton and NH₄⁺ flux in the root tip based on a previous study by Xu et al. (2013).

3-day old rice (~ 3 cm long seminal root) and Arabidopsis roots (~ 2 cm long primary root) were treated in N-free (-N) or NH₄⁺ medium with or without supplying MES. Subsequently, the roots were placed in Petri dishes containing 20 ml of same liquid medium. The surface of the roots needs to be cleaned gently with a soft brush in time to prevent surface attachments from affecting experimental results. The H⁺ and NH₄⁺ fluxes of rice plants were measured along the root tip, concentrating on the following zones: 0, 150, 300, 600, 1200, 1800 and 2400 μm from the root cap junction. The microelectrodes were positioned 0 ± 2 μm away from the samples by the computer-controlled NMT system, each position of the sample was measured for 3 to 5 minutes.

Plasmid Construction and Plant Transformation

To generate transgenic rice *pOsAMT1;1:nls-GUS* reporter line, ~2 kb upstream of the start codon of *OsAMT1;1* was amplified, and subcloned into the expression vector pMK7SNFm14GW,0 by using Gateway cloning system. Primers used are listed below: Forward primer:

GGGGACAACCTTTGTATAGAAAAGTTGCGGGCTGCTTGCAGGAATGTAT; Reverse primer: GGGGACTGCTTTTTTTGTACAAACTTGTCTTCCTCCCTCCCTCACCAA

The construct was further transformed into the calluses of *Oryza sativa.L.*, cultivars Nipponbare via *Agrobacterium tumefaciens* as described previously (Hiei *et al.* 1994).

Histochemical analysis of β -Glucuronidase (GUS) expression

The GUS staining of the root tissues of transgenic *pOsAMT1;1:nls-GUS* line was performed as described previously (Xuan *et al.* 2015). The root tissues from 7-day-old seedlings were cleared by mounting in 90% (v/v) lactic acid before imaging with microscopy (Leica DM2500).

Confocal Microscopy

DR5rev:VENUS-N7 and *DII-VENUS* expression in the root tip of rice and Arabidopsis was acquired with a Leica SP8 laser-scanning microscope equipped with white laser and hybrid laser detector. The root tips of Arabidopsis *DR5rev:3xVENUS-N7* transgenic seedlings were directly imaged after being treated for the indicated time, whereas the root tips of rice *DR5rev:3xVENUS-N7* transgenic seedlings from different treatments were cleaned with a modified ClearSee method preceding confocal imaging (Kurihara *et al.* 2015). Briefly, rice roots grown upon different treatments were harvested and fixed with 4% paraformaldehyde in PBS for 1 hour at room temperature with gentle agitation, followed by 4 hour of vacuum treatment. Subsequently, the root samples were washed twice with PBS (1 min each time), and then incubated in ClearSee solution at room temperature with gentle agitation for 1d. *DR5rev:3xVENUS-N7* signal intensity in the outer layer of lateral root cap and epidermal cells on a median confocal optical section image was measured.

PI and MPS-PI staining

For the propidium iodide (PI)-treated Arabidopsis root images, after treatment for indicated time, the Arabidopsis seedlings were stained with 2 μ g/mL PI for 3 minutes, washed with distilled water, and used for confocal imaging.

MPS-PI staining was used for the cleaning and visualization of cell organization of rice seminal root tip. After treatment for indicated time, rice seminal root tips (~2 cm) were harvested and fixed in 50% methanol and 10% acetic acid for 12 hours in 4 °C, then rinsed with water and submerged in 1% periodic acid for 40 minutes at room temperature. After rinsing with water again, root tip samples were stained with PI (100 ug/mL) and mounted onto microscopic slides and covered with chloral hydrate solution clearing buffer overnight (4 g chloral hydrate, 1 mL glycerol, 2 mL water). Subsequently, excess chloral hydrate was removed and several drops of Hoyer's solution was added to the root sample before covered with a slide. The slides were further leaved undisturbed for 3 days to allow setting of the mounting medium, and then taken for confocal imaging.

For both rice and Arabidopsis, the root meristem length and cortical cell number of each individual root were measured.

Data analyses

The experiments performed in this study were repeated at least three times, and all the results are presented as the mean \pm standard deviation (s.d.). SPSS software was used for statistical analysis.

The significant difference between two sets of data was performed by Student's *t*-test, whereas the difference among more than two sets of data were analyzed with one-way ANOVA and Duncan's multiple comparison.

DATA AVAILABILITY STATEMENT

All relevant data generated during this study can be found within the manuscript and its supplemental information files. Materials are also available from the corresponding author upon request.

ACKNOWLEDGEMENTS

We thank Prof. Dabing Zhang (Shanghai Jiao Tong University) for provide rice

DR5rev:3xVENUS-N7 reporter line, Prof. Nicolaus von Wirén (Leibniz Institute of Plant Genetics

and Crop Plant Research, Germany) for providing *AMT qko* mutant, Prof. Claus Schwechheimer (Technische Universität München, Germany) for providing *d6pk013* mutant, and Prof. Qun Zhang (Nanjing Agricultural University) for providing *pid* mutant. We also thank experiment technician Jin Wang (Centre of life science in Nanjing Agricultural University) for guiding the NMT experiments, and Caihong Song for vector construction.

AUTHOR CONTRIBUTIONS

W.X. and T.B. directed the experiments. L.J., Y.X., and Z.W. performed most of the experiments and analysis. L.L. and C.Z. helped with quantification of root phenotype. P. P., B.P., and W.Q. helped with data analysis. W.X. and T.B. wrote the manuscript. All authors discussed the results and contributed in the finalization of the manuscript.

FUNDING

This work was supported by China National Key Program for Research and Development (2016YFD0100700), Research Foundation – Flanders (FWO, Belgium), Bilateral Research Cooperation with MOST (China) (2016YFE0109900), National Natural Science Foundation (No. 31672223 and 31822047), the Fundamental Research Funds for the Central Universities (KJYQ201903 and KYT201802), Innovative Research Team Development Plan of the Ministry of Education of China (No. IRT_17R56), Innovative Scientific and Technological Talents in Henan Province (20HASTIT041) and the 111 Project (D16014).

CONFLICT OF INTEREST

The authors declare no conflict of interest.

SUPPORTING INFORMATION

Additional Supporting Information may be found in the online version of this manuscript.

Figure S1. The effects of different nitrogen forms on rice shoot and root development.

Figure S2. The effects of NH_4^+ on rice root meristem length and cortical cell number.

Figure S3. The effects of NH_4^+ on rice root development in solid agar medium.

Figure S4. Adventitious and lateral roots of rice NIP seedlings show a helical growth pattern in NH_4^+ treatments.

Figure S5. The effects of NH_4^+ on the root development of knock-out mutants and overexpression lines of *OsAMT1;1*.

Figure S6. Expression pattern of *OsAMT1.1* in rice root.

Figure S7. NH_4^+ treatment leads to the acidification of the rice medium.

Figure S8. The effects of DCCD on the NH_4^+ -induced root development and medium acidification.

Figure S9. Low pH results in shorter seminal roots and a helical root growth response regardless of NH_4^+ supplies.

Figure S10. MES suppresses NH_4^+ -induced root responses in rice.

Figure S11. Auxin inhibitors alleviate the helical root response of rice seminal root, under NH_4^+ treatment.

Figure S12. The effects of NH_4^+ and NO_3^- on Arabidopsis root elongation and root acidification.

Figure S13. NH_4^+ -repressed Arabidopsis root elongation is alleviated by MES.

Figure S14: The effects of NH_4^+ on Arabidopsis root meristem length and cortical cell number.

Figure S15. The effects of NH_4^+ on the DR5 expression pattern in the root tip and the root development of various auxin mutants.

Figure S16. The effects of NAA, IAA, and NAA on DII expression under NH_4^+ and acidic stress in Arabidopsis.

Movie S1. Movie of the root tips of rice NIP seedlings grown in N-free and NH_4^+ -containing medium in the absence or presence of MES over 60 hours since treatment.

Movie S2. Movie of indicated rice cultured mediums that supplied with pH indicator BCP (0.006% w/v) over 47 hours since treatment.

Movie S3. Movie of indicated rice cultured mediums that supplied with pH indicator BCP (0.006% w/v) over 47 hours since treatment.

References

- Adamowski, M. and Friml, J.** (2015) PIN-dependent auxin transport: action, regulation, and evolution. *The Plant cell*, **27**, 20-32.
- Araya, T., Miyamoto, M., Wibowo, J., Suzuki, A., Kojima, S., Tsuchiya, Y.N., Sawa, S., Fukuda, H., von Wieren, N. and Takahashi, H.** (2014) CLE-CLAVATA1 peptide-receptor signaling module regulates the expansion of plant root systems in a nitrogen-dependent manner. *Proceedings of the National Academy of Sciences of the United States of America*, **111**, 2029-2034.
- Band, L.R., Wells, D.M., Larrieu, A., Sun, J.Y., Middleton, A.M., French, A.P., Brunoud, G., Sato, E.M., Wilson, M.H., Peret, B., Oliva, M., Swarup, R., Sairanen, I., Parry, G., Ljung, K., Beeckman, T., Garibaldi, J.M., Estelle, M., Owen, M.R., Vissenberg, K., Hodgman, T.C., Pridmore, T.P., King, J.R., Vernoux, T. and Bennett, M.J.** (2012) Root gravitropism is regulated by a transient lateral auxin gradient controlled by a tipping-point mechanism. *Proceedings of the National Academy of Sciences of the United States of America*, **109**, 4668-4673.
- Barbez, E., Dunser, K., Gaidora, A., Lendl, T. and Busch, W.** (2017) Auxin steers root cell expansion via apoplastic pH regulation in Arabidopsis thaliana. *Proc Natl Acad Sci U S A*, **114**, E4884-E4893.
- Baster, P., Robert, S., Kleine-Vehn, J., Vanneste, S., Kania, U., Grunewald, W., De Rybel, B., Beeckman, T. and Friml, J.** (2013) SCF(TIR1/AFB)-auxin signalling regulates PIN vacuolar trafficking and auxin fluxes during root gravitropism. *Embo J*, **32**, 260-274.
- Brunoud, G., Wells, D.M., Oliva, M., Larrieu, A., Mirabet, V., Burrow, A.H., Beeckman, T., Kepinski, S., Traas, J., Bennett, M.J. and Vernoux, T.** (2012) A novel sensor to map auxin response and distribution at high spatio-temporal resolution. *Nature*, **482**, 103-U132.
- Cao, Y.W., Glass, A.D.M. and Crawford, N.M.** (1993) Ammonium Inhibition Of Arabidopsis Root-Growth Can Be Reversed by Potassium And by Auxin Resistance Mutations Aux1, Axr1, And Axr2. *Plant physiology*, **102**, 983-989.
- Dang, X., Chen, B., Liu, F., Ren, H., Liu, X., Zhou, J., Qin, Y. and Lin, D.** (2020) Auxin

Signaling-Mediated Apoplastic pH Modification Functions in Petal Conical Cell Shaping. *Cell reports*, **30**, 3904-3916 e3903.

Delbarre, A., Muller, P., Imhoff, V. and Guern, J. (1996) Comparison of mechanisms controlling uptake and accumulation of 2,4-dichlorophenoxy acetic acid, naphthalene-1-acetic acid, and indole-3-acetic acid in suspension-cultured tobacco cells. *Planta*, **198**, 532-541.

Di, D.W., Sun, L., Zhang, X.N., Li, G.J., Kronzucker, H.J. and Shi, W.M. (2018) Involvement of auxin in the regulation of ammonium tolerance in rice (*Oryza sativa* L.). *Plant Soil*, **432**, 373-387.

Dindas, J., Becker, D., Roelfsema, M.R.G., Scherzer, S., Bennett, M. and Hedrich, R. (2020) Pitfalls in auxin pharmacology. *The New phytologist*, **227**, 286-292.

Fendrych, M., Leung, J. and Friml, J. (2016) TIR1/AFB-Aux/IAA auxin perception mediates rapid cell wall acidification and growth of *Arabidopsis* hypocotyls. *Elife*, **5**.

Feng, W., Lindner, H., Robbins, N.E., 2nd and Dinneny, J.R. (2016) Growing Out of Stress: The Role of Cell- and Organ-Scale Growth Control in Plant Water-Stress Responses. *The Plant cell*, **28**, 1769-1782.

Fukaki, H., Tameda, S., Masuda, H. and Tasaka, M. (2002) Lateral root formation is blocked by a gain-of-function mutation in the SOLITARY-ROOT/IAA14 gene of *Arabidopsis*. *Plant Journal*, **29**, 153-168.

Gaudinier, A., Rodriguez-Medina, J., Zhang, L., Olson, A., Liseron-Monfils, C., Bagman, A.M., Foret, J., Abbitt, S., Tang, M., Li, B., Runcie, D.E., Kliebenstein, D.J., Shen, B., Frank, M.J., Ware, D. and Brady, S.M. (2018) Transcriptional regulation of nitrogen-associated metabolism and growth. *Nature*, **563**, 259-264.

Giehl, R.F. and von Wiren, N. (2014) Root nutrient foraging. *Plant physiology*, **166**, 509-517.

Gujas, B., Alonso-Blanco, C. and Hardtke, C.S. (2012) Natural *Arabidopsis* brx loss-of-function alleles confer root adaptation to acidic soil. *Current biology : CB*, **22**, 1962-1968.

Gutknecht, J. and Walter, A. (1980) Transport of auxin (indoleacetic acid) through lipid bilayer

membranes. *The Journal of Membrane Biology*, **56**, 65-72.

Hayashi, K., Neve, J., Hirose, M., Kuboki, A., Shimada, Y., Kepinski, S. and Nozaki, H. (2012) Rational Design of an Auxin Antagonist of the SCFTIR1 Auxin Receptor Complex.

Acs Chem Biol, **7**, 590-598.

Henrichs, S., Wang, B.J., Fukao, Y., Zhu, J.S., Charrier, L., Bailly, A., Oehring, S.C., Linnert, M., Weiwad, M., Endler, A., Nanni, P., Pollmann, S., Mancuso, S., Schulz, A. and Geisler, M. (2012) Regulation of ABCB1/PGP1-catalysed auxin transport by linker phosphorylation. *Embo J*, **31**, 2965-2980.

Hiei, Y., Ohta, S., Komari, T. and Kumashiro, T. (1994) Efficient transformation of rice (*Oryza sativa* L.) mediated by *Agrobacterium* and sequence analysis of the boundaries of the T-DNA. *The Plant journal : for cell and molecular biology*, **6**, 271-282.

Hirano, T., Satoh, Y., Ohki, A., Takada, R., Arai, T. and Michiyama, H. (2008) Inhibition of ammonium assimilation restores elongation of seminal rice roots repressed by high levels of exogenous ammonium. *Physiol Plantarum*, **134**, 183-190.

Jia, Z., Giehl, R.F.H., Meyer, R.C., Altmann, T. and von Wiren, N. (2019) Natural variation of BSK3 tunes brassinosteroid signaling to regulate root foraging under low nitrogen. *Nature communications*, **10**, 2378.

Jiao, X., Wang, H., Yan, J., Kong, X., Liu, Y., Chu, J., Chen, X., Fang, R. and Yan, Y. (2019) Promotion of BR biosynthesis by miR444 is required for ammonium-triggered inhibition of root growth. *Plant physiology*, pp.00190.02019.

Kim, J.Y., Henrichs, S., Bailly, A., Vincenzetti, V., Sovero, V., Mancuso, S., Pollmann, S., Kim, D., Geisler, M. and Nam, H.G. (2010) Identification of an ABCB/P-glycoprotein-specific Inhibitor of Auxin Transport by Chemical Genomics. *Journal Of Biological Chemistry*, **285**, 23307-23315.

Korver, R.A., Koevoets, I.T. and Testerink, C. (2018) Out of Shape During Stress: A Key Role for Auxin. *Trends Plant Sci*, **23**, 783-793.

Krouk, G., Lacombe, B., Bielach, A., Perrine-Walker, F., Malinska, K., Mounier, E., Hoyerova, K., Tillard, P., Leon, S., Ljung, K., Zazimalova, E., Benkova, E., Nacry, P.

-
- and Gojon, A.** (2010) Nitrate-regulated auxin transport by NRT1.1 defines a mechanism for nutrient sensing in plants. *Developmental cell*, **18**, 927-937.
- Kurihara, D., Mizuta, Y., Sato, Y. and Higashiyama, T.** (2015) ClearSee: a rapid optical clearing reagent for whole-plant fluorescence imaging. *Development*, **142**, 4168-4179.
- Li, B., Li, G., Kronzucker, H.J., Baluska, F. and Shi, W.** (2014a) Ammonium stress in Arabidopsis: signaling, genetic loci, and physiological targets. *Trends Plant Sci*, **19**, 107-114.
- Li, B.H., Li, G.J., Kronzucker, H.J., Baluska, F. and Shi, W.M.** (2014b) Ammonium stress in Arabidopsis: signaling, genetic loci, and physiological targets. *Trends Plant Sci*, **19**, 107-114.
- Li, C., Tang, Z., Wei, J., Qu, H., Xie, Y. and Xu, G.** (2016) The OsAMT1.1 gene functions in ammonium uptake and ammonium-potassium homeostasis over low and high ammonium concentration ranges. *Journal of genetics and genomics = Yi chuan xue bao*, **43**, 639-649.
- Lima, J.E., Kojima, S., Takahashi, H. and von Wiren, N.** (2010) Ammonium Triggers Lateral Root Branching in Arabidopsis in an AMMONIUM TRANSPORTER1;3-Dependent Manner. *The Plant cell*, **22**, 3621-3633.
- Liu, K.H., Niu, Y., Konishi, M., Wu, Y., Du, H., Sun Chung, H., Li, L., Boudsocq, M., McCormack, M., Maekawa, S., Ishida, T., Zhang, C., Shokat, K., Yanagisawa, S. and Sheen, J.** (2017) Discovery of nitrate-CPK-NLP signalling in central nutrient-growth networks. *Nature*, **545**, 311-316.
- Loque, D. and von Wiren, N.** (2004) Regulatory levels for the transport of ammonium in plant roots. *Journal of experimental botany*, **55**, 1293-1305.
- Luo, L., Wang, H., Liu, X., Hu, J., Zhu, X., Pan, S., Qin, R., Wang, Y., Zhao, P., Fan, X. and Xu, G.** (2018) Strigolactones affect the translocation of nitrogen in rice. *Plant science : an international journal of experimental plant biology*, **270**, 190-197.
- Meng, F., Xiang, D., Zhu, J., Li, Y. and Mao, C.** (2019) Molecular Mechanisms of Root Development in Rice. *Rice*, **12**, 1.
- Michniewicz, M., Brewer, P.B. and Friml, J.** (2007) Polar Auxin Transport and Asymmetric

Auxin Distribution. *The Arabidopsis Book*.

Muller, A., Guan, C.H., Galweiler, L., Tanzler, P., Huijser, P., Marchant, A., Parry, G., Bennett, M., Wisman, E. and Palme, K. (1998) AtPIN2 defines a locus of Arabidopsis for root gravitropism control. *Embo J*, **17**, 6903-6911.

Nishimura, T., Hayashi, K., Suzuki, H., Gyohda, A., Takaoka, C., Sakaguchi, Y., Matsumoto, S., Kasahara, H., Sakai, T., Kato, J., Kamiya, Y. and Koshiba, T. (2014) Yucasin is a potent inhibitor of YUCCA, a key enzyme in auxin biosynthesis. *Plant Journal*, **77**, 352-366.

O'Brien, J.A., Vega, A., Bouguyon, E., Krouk, G., Gojon, A., Coruzzi, G. and Gutierrez, R.A. (2016) Nitrate Transport, Sensing, and Responses in Plants. *Molecular plant*, **9**, 837-856.

Ohkubo, Y., Tanaka, M., Tabata, R., Ogawa-Ohnishi, M. and Matsubayashi, Y. (2017) Shoot-to-root mobile polypeptides involved in systemic regulation of nitrogen acquisition. *Nat Plants*, **3**, 17029.

Okushima, Y., Overvoorde, P.J., Arima, K., Alonso, J.M., Chan, A., Chang, C., Ecker, J.R., Hughes, B., Lui, A., Nguyen, D., Onodera, C., Quach, H., Smith, A., Yu, G.X. and Theologis, A. (2005) Functional genomic analysis of the AUXIN RESPONSE FACTOR gene family members in Arabidopsis thaliana: Unique and overlapping functions of ARF7 and ARF19. *The Plant cell*, **17**, 444-463.

Orman-Ligeza, B., Morris, E.C., Parizot, B., Lavigne, T., Babe, A., Ligeza, A., Klein, S., Sturrock, C., Xuan, W., Novak, O., Ljung, K., Fernandez, M.A., Rodriguez, P.L., Dodd, I.C., De Smet, I., Chaumont, F., Batoko, H., Perilleux, C., Lynch, J.P., Bennett, M.J., Beeckman, T. and Draye, X. (2018) The Xerobranching Response Represses Lateral Root Formation When Roots Are Not in Contact with Water. *Current biology : CB*, **28**, 3165-3173 e3165.

Ortiz-Ramirez, C., Mora, S.I., Trejo, J. and Pantoja, O. (2011) PvAMT1;1, a highly selective ammonium transporter that functions as H⁺/NH₄⁽⁺⁾ symporter. *The Journal of biological chemistry*, **286**, 31113-31122.

-
- Pacheco-Villalobos, D., Diaz-Moreno, S.M., van der Schuren, A., Tamaki, T., Kang, Y.H., Gujas, B., Novak, O., Jaspert, N., Li, Z., Wolf, S., Oecking, C., Ljung, K., Bulone, V. and Hardtke, C.S.** (2016) The Effects of High Steady State Auxin Levels on Root Cell Elongation in *Brachypodium*. *The Plant cell*, **28**, 1009-1024.
- Parry, G., Calderon-Villalobos, L.I., Prigge, M., Peret, B., Dharmasiri, S., Itoh, H., Lechner, E., Gray, W.M., Bennett, M. and Estelle, M.** (2009) Complex regulation of the TIR1/AFB family of auxin receptors. *Proceedings of the National Academy of Sciences of the United States of America*, **106**, 22540-22545.
- Parry, G., Delbarre, A., Marchant, A., Swarup, R., Napier, R., Perrot-Rechenmann, C. and Bennett, M.J.** (2001) Novel auxin transport inhibitors phenocopy the auxin influx carrier mutation *aux1*. *The Plant journal : for cell and molecular biology*, **25**, 399-406.
- Poitout, A., Crabos, A., Petrik, I., Novak, O., Krouk, G., Lacombe, B. and Ruffel, S.** (2018) Responses to Systemic Nitrogen Signaling in Arabidopsis Roots Involve trans-Zeatin in Shoots. *The Plant cell*, **30**, 1243-1257.
- Straub, T., Ludewig, U. and Neuhauser, B.** (2017) The Kinase CIPK23 Inhibits Ammonium Transport in Arabidopsis thaliana. *The Plant cell*, **29**, 409-422.
- Swarup, R., Kargul, J., Marchant, A., Zadik, D., Rahman, A., Mills, R., Yemm, A., May, S., Williams, L., Millner, P., Tsurumi, S., Moore, I., Napier, R., Kerr, I.D. and Bennett, M.J.** (2004) Structure-function analysis of the presumptive Arabidopsis auxin permease AUX1. *The Plant cell*, **16**, 3069-3083.
- Swarup, R., Kramer, E.M., Perry, P., Knox, K., Leyser, H.M., Haseloff, J., Beemster, G.T., Bhalerao, R. and Bennett, M.J.** (2005) Root gravitropism requires lateral root cap and epidermal cells for transport and response to a mobile auxin signal. *Nature cell biology*, **7**, 1057-1065.
- Swarup, R. and Peret, B.** (2012) AUX/LAX family of auxin influx carriers-an overview. *Frontiers in plant science*, **3**.
- Tabata, R., Sumida, K., Yoshii, T., Ohyama, K., Shinohara, H. and Matsubayashi, Y.** (2014) Perception of root-derived peptides by shoot LRR-RKs mediates systemic N-demand

signaling. *Science*, **346**, 343-346.

Teale, W. and Palme, K. (2018) Naphthylphthalamic acid and the mechanism of polar auxin transport. *Journal of experimental botany*, **69**, 303-312.

Wang, W., Hu, B., Yuan, D., Liu, Y., Che, R., Hu, Y., Ou, S., Liu, Y., Zhang, Z., Wang, H., Li, H., Jiang, Z., Zhang, Z., Gao, X., Qiu, Y., Meng, X., Liu, Y., Bai, Y., Liang, Y., Wang, Y., Zhang, L., Li, L., Sodmergen, Jing, H., Li, J. and Chu, C. (2018) Expression of the Nitrate Transporter Gene OsNRT1.1A/OsNPF6.3 Confers High Yield and Early Maturation in Rice. *The Plant cell*, **30**, 638-651.

Wang, Y., Gong, Z., Friml, J. and Zhang, J. (2019) Nitrate Modulates the Differentiation of Root Distal Stem Cells. *Plant physiology*, **180**, 22-25.

Xuan, W., Audenaert, D., Parizot, B., Moller, B.K., Njo, M.F., De Rybel, B., De Rop, G., Van Isterdael, G., Mahonen, A.P., Vanneste, S. and Beeckman, T. (2015) Root Cap-Derived Auxin Pre-patterns the Longitudinal Axis of the Arabidopsis Root. *Current biology : CB*, **25**, 1381-1388.

Xuan, W., Band, L.R., Kumpf, R.P., Van Damme, D., Parizot, B., De Rop, G., Opendacker, D., Moller, B.K., Skorzinski, N., Njo, M.F., De Rybel, B., Audenaert, D., Nowack, M.K., Vanneste, S. and Beeckman, T. (2016) Cyclic programmed cell death stimulates hormone signaling and root development in Arabidopsis. *Science*, **351**, 384-387.

Xuan, W., Beeckman, T. and Xu, G. (2017) Plant nitrogen nutrition: sensing and signaling. *Current opinion in plant biology*, **39**, 57-65.

Xuan, Y.H., Priatama, R.A., Huang, J., Je, B.I., Liu, J.M., Park, S.J., Piao, H.L., Son, D.Y., Lee, J.J., Park, S.H., Jung, K.H., Kim, T.H. and Han, C.D. (2013) Indeterminate domain 10 regulates ammonium-mediated gene expression in rice roots. *The New phytologist*, **197**, 791-804.

Yan, F., Feuerle, R., Schaffer, S., Fortmeier, H. and Schubert, S. (1998) Adaptation of active proton pumping and plasmalemma ATPase activity of corn roots to low root medium pH. *Plant physiology*, **117**, 311-319.

Yang, J., Yuan, Z., Meng, Q., Huang, G., Perin, C., Bureau, C., Meunier, A.C., Ingouff, M.,

Bennett, M.J., Liang, W. and Zhang, D. (2017) Dynamic Regulation of Auxin Response during Rice Development Revealed by Newly Established Hormone Biosensor Markers. *Frontiers in plant science*, **8**, 256.

Zhang, Y.Z., He, P., Ma, X.F., Yang, Z.R., Pang, C.Y., Yu, J.N., Wang, G.D., Friml, J. and Xiao, G.H. (2019a) Auxin-mediated statolith production for root gravitropism. *New Phytologist*, **224**, 761-774.

Zhang, Y.Z., Xiao, G.H., Wang, X.J., Zhang, X.X. and Friml, J. (2019b) Evolution of fast root gravitropism in seed plants. *Nature communications*, **10**.

Zhu, Y., Di, T., Xu, G., Chen, X., Zeng, H., Yan, F. and Shen, Q. (2009) Adaptation of plasma membrane H(+)-ATPase of rice roots to low pH as related to ammonium nutrition. *Plant, cell & environment*, **32**, 1428-1440.

Zou, N., Li, B.H., Dong, G.Q., Kronzucker, H.J. and Shi, W.M. (2012) Ammonium-induced loss of root gravitropism is related to auxin distribution and TRH1 function, and is uncoupled from the inhibition of root elongation in Arabidopsis. *Journal of experimental botany*, **63**, 3777-3788.

Zourelidou, M., Muller, I., Willige, B.C., Nill, C., Jikumaru, Y., Li, H.B. and Schwechheimer, C. (2009) The polarly localized D6 PROTEIN KINASE is required for efficient auxin transport in Arabidopsis thaliana. *Development*, **136**, 627-636.

Figure Legends

Figure 1: Ammonium nitrogen triggers a helical root growth response and the acidification of the rice roots.

- (a) Root phenotype of rice NIP seedlings grown in medium supplied with different N donors for 4 days. Lower panels are close-ups of a representative root tip of one seedling shown in the upper panel. The white dotted line indicates the position of the root tip when the seedlings were transferred to media supplied with different nitrogen donors.
- (b) Quantification of seminal root (SR) elongation and root helical index of rice NIP seedlings under different treatments shown in (a) (n = 10 seedlings).
- (c) Quantification of root tip angles relative to the medial axis in rice seedlings untreated or treated with NH_4^+ over 48 hours. Red arrow indicates the time-point when the root tip loses the sensitivity to gravity.
- (d) Root phenotype of NIP and *pUBI:AMT1;1* transgenic rice seedlings in medium supplied with or without NH_4^+ for 24 hours (also see Supplemental Fig. 5c).
- (e) Quantification of seminal root elongation and helical index of rice NIP seedlings shown in f (n = 10 seedlings). Scale bar, 0.5 cm.

For the SR elongation, only the SR segment newly formed during the 4-day treatment was quantified. All the data represent means \pm s.d., and the letters above the plots indicate significant differences among treatments ($P < 0.05$ by one-way ANOVA and Duncan's multiple comparison).

Yellow scale bar, 2 cm; white scale bars, 0.5 cm.

Figure 2: Ammonium supply triggers proton fluxes in the root tip and root acidification.

- (a) Quantification of the net NH_4^+ and proton fluxes in the root tip of rice NIP seedlings treated with varying NH_4^+ concentrations in the absence or presence of MES (n = 3 seedlings).
- (b) Root acidification under N-free and NH_4^+ treatments as revealed by staining equal amount of the root tip segments of seedlings with BCP for indicated time points (n = 5 seedlings).
- (c and d) Root tip phenotype (c) and quantification (d) of root helical index of rice NIP seedlings grown in N-free and NH_4^+ -supplied medium supplied with 1 mM DCCD (n = 10 seedlings).
- (e) Measurement of pH of the N-free and NH_4^+ -containing medium supplied with or without 1 μM DCCD over 2 days (n = 3 pots).

All the data represent the means \pm s.d., and the letters above the plots indicate significant differences among treatments ($P < 0.05$ by one-way ANOVA and Duncan's multiple comparison).
white scale bar, 0.5 cm.

Figure 3: Ammonium-induced medium acidification and helical root response are repressed when medium pH is buffered.

(a) Medium acidification after 48 hours treatment as revealed by adding BCP (0.006 % w/v) in the rice-cultured medium since the onset of the treatments.

(b) Root phenotype of N-free and NH_4^+ -treated NIP seedlings in the absence or presence of MES after 4 days of treatment. Lower panel are the close-ups the root tip of one representative seedling shown in the upper panel. The white dotted line indicates the root tip position when the seedlings were transferred to different media.

(c) Quantification of SR elongation and gravitropic index of NIP rice seedlings under different treatments shown in (b) (n = 10 seedlings). For the SR elongation, only the SR segment newly formed during the 4-day treatment was quantified.

All the data represent means \pm s.d.. The letters above the plots indicate significant differences among treatments ($P < 0.05$ by one-way ANOVA and Duncan's multiple comparison). Black scale bar, 4 cm; white scale bars, 0.5 cm.

Figure 4: Auxin mediates the NH₄⁺-triggered root helical growth response.

(a) Root phenotype (upper panel, 4-day treatment) and the expression pattern of *DR5rev:3xVENUS-N7* (lower panel, 36-h treatment) at the root tip of rice (cv. 9322) seedlings upon indicated treatments for 4 days and 36 hours, respectively.

(b) Quantification of root helical index of rice (cv. 9322) seedlings under different treatments shown in **(a)** (n = 10 seedlings).

(c) Quantification of *DR5rev:3xVENUS-N7* in LRC and epidermal cell layers at the root tip upon different treatments shown in **(a)** (n = 10 seedlings).

(d) Root phenotype (upper panel, 4-days of treatment) and the expression pattern of *DR5rev:3xVENUS-N7* (lower panel, 36-h treatment) at the root tip of rice seedlings upon treatment with indicated auxin inhibitors for 4 days and 36 hours, respectively.

(e) Quantification of root gravitropic index of rice seedlings under indicated treatments shown in **(d)** (n = 10 seedlings).

(f) Quantification of *DR5rev:3xVENUS-N7* signal in LRC and epidermal cell layers at the root tip of rice seedlings under indicated treatments in **(d)** (n = 10 seedlings).

(g) Medium acidification after 48 hours treatments of indicated auxin inhibitors as revealed by adding pH indicator BCP in the rice-cultured medium since the onset of the treatments. NPA, BUM, NOA, PEO-IAA, and YUCASIN were used at 0.1 μM, 1 μM, 0.1 μM, 5 μM, and 5 μM, respectively.

(h) Quantification of pH of the NH₄⁺-containing medium supplied with different inhibitors over 4 days (n = 3 pots). Medium was refreshed every 2 days with pH adjusted to 5.5.

White triangle shown in **(a)** and **(d)** indicates asymmetric *DR5* accumulation in the LRC and epidermis. a.u., arbitrary units. All the data represent means ±s.d.. Asterisk indicates significant differences ($P < 0.05$ by Student's t-test), and the letters above the plots indicate significant differences among treatments ($P < 0.05$ by one-way ANOVA and Duncan's multiple comparison).

White scale bars, 0.5 cm; red scale bars, 200 μm; Black scale bar, 4 cm.

Figure 5: NH₄⁺ regulates Arabidopsis root elongation through acidification of root cells but independently of auxin signaling.

(a) Root phenotype of 3-day-old Col-0 and *qko* mutant seedlings under different treatments for another 3 days. The white dotted lines indicate the root tip position when the seedlings were transferred to different mediums.

(b and c), Quantification of PR elongation and root tip angles of Col-0 and *qko* seedlings with respect to different treatments shown in **a** (n = 10 seedlings). For the PR elongation, only the PR segment newly formed during the 3-day treatment was quantified.

(d) Quantification of the net NH₄⁺ and proton fluxes in the root tip of 3-day-old Col-0 and *qko* mutant seedlings treated with or without NH₄⁺ in the absence of MES (n = 3 seedlings)

(e) Quantification of the proton fluxes in the root tip of 3-day-old Col-0 and *qko* mutant seedlings under low pH (n = 3 seedlings).

(f and g), Expression and quantification of DII-VENUS signal in the root tip of Col-0 and *aux1-21* seedlings after 48-h treatment. The DII-VENUS signals in the LRC and epidermis (EP) and stele were measured and represented respectively in **(g)** (n = 10 seedlings). a.u., arbitrary units.

All the data represent means ±s.d., and the letters above the plots indicate significant differences among treatments ($P < 0.05$ by one-way ANOVA and Duncan's multiple comparison). White scale bar, 1 cm; yellow scale bar, 100 μm.

Figure 6: NH₄⁺- and low pH-regulated seminal root elongation and helical root response are reversible in rice rather than Arabidopsis.

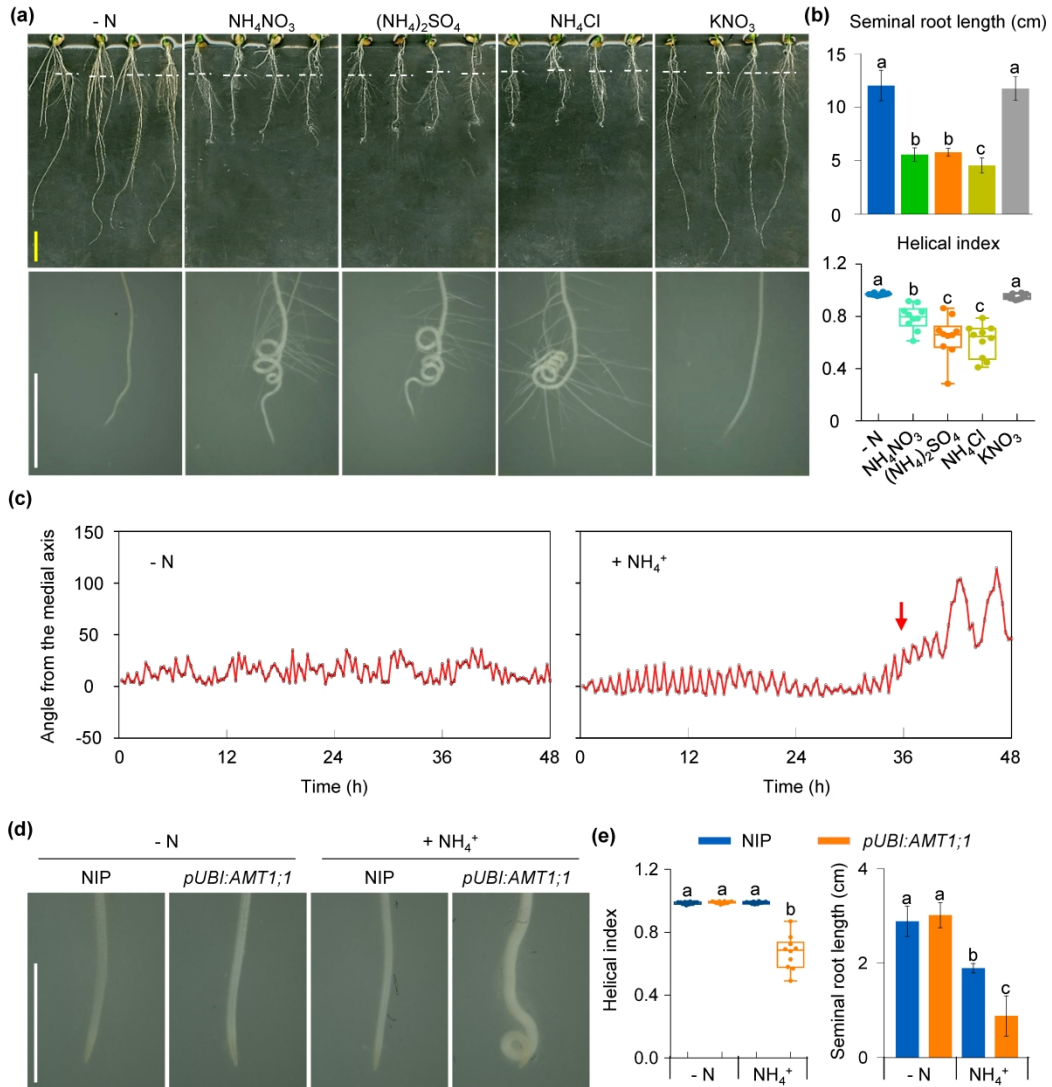
(a) Root phenotype of rice NIP seedlings first grown in MES-free or pH 4 medium for 2 days, and then respectively transferred to MES supplied or pH 5.5 medium for another 2 days. White dashed lines indicate the root tip position when the seedlings were transferred for indicated treatments. Lower panels are close-ups of the root tips inside the white boxed area in the upper panel. Yellow arrows indicate the restore of SR elongation after transfer.

(b) Quantification of SR length and root helical index of rice NIP seedlings under different treatments shown in **A** (n = 10 seedlings).

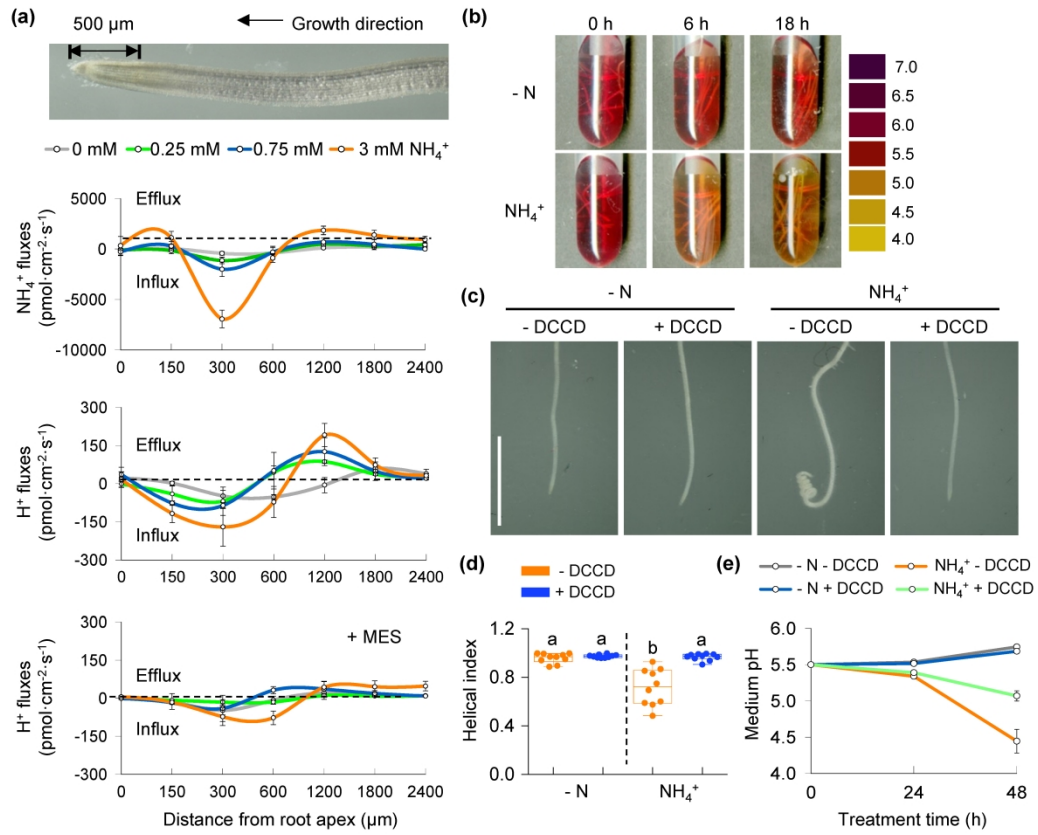
(c) Root phenotype of NH₄⁺-treated Arabidopsis Col-0 seedlings after being transferred from MES-free medium to MES supplied medium, or from low pH medium (pH = 5) to control medium (pH = 5.8) for another 3 days. White dashed lines indicate the root tip position at the onset of the treatments. Lower panels are close-ups of the root tips inside the white boxed area in the upper panel.

(d) Quantification of PR length of Arabidopsis Col-0 seedlings under different treatments shown in **(c)** (n = 10 seedlings).

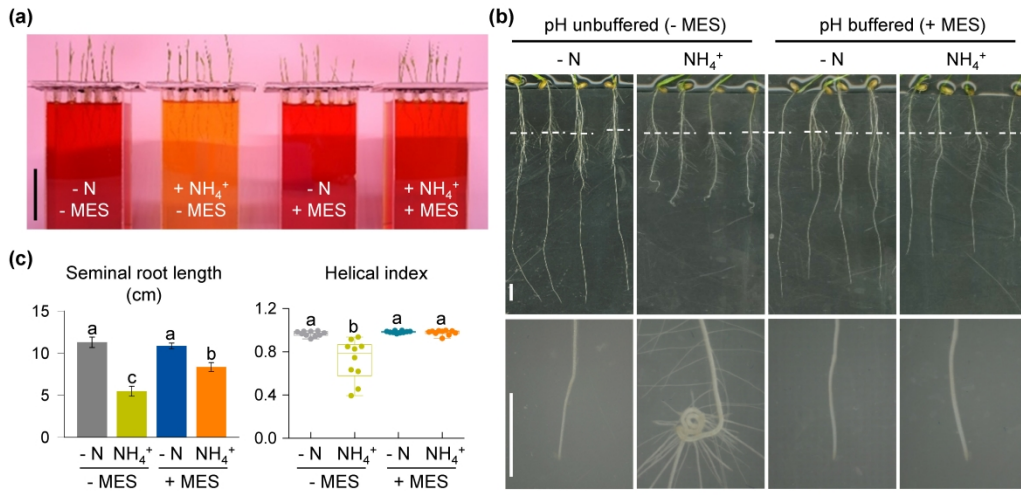
The SR (rice) and PR (Arabidopsis) root segments newly formed after transfer was quantified. The % reduction in root length is indicated in **(b)** and **(d)**. Data represent the means ± s.d, and the letters above the plots indicate significant differences among treatments ($P < 0.05$ by one-way ANOVA and Duncan's multiple comparison). Black scale bar, 2 cm; white scale bars, 0.5 cm.



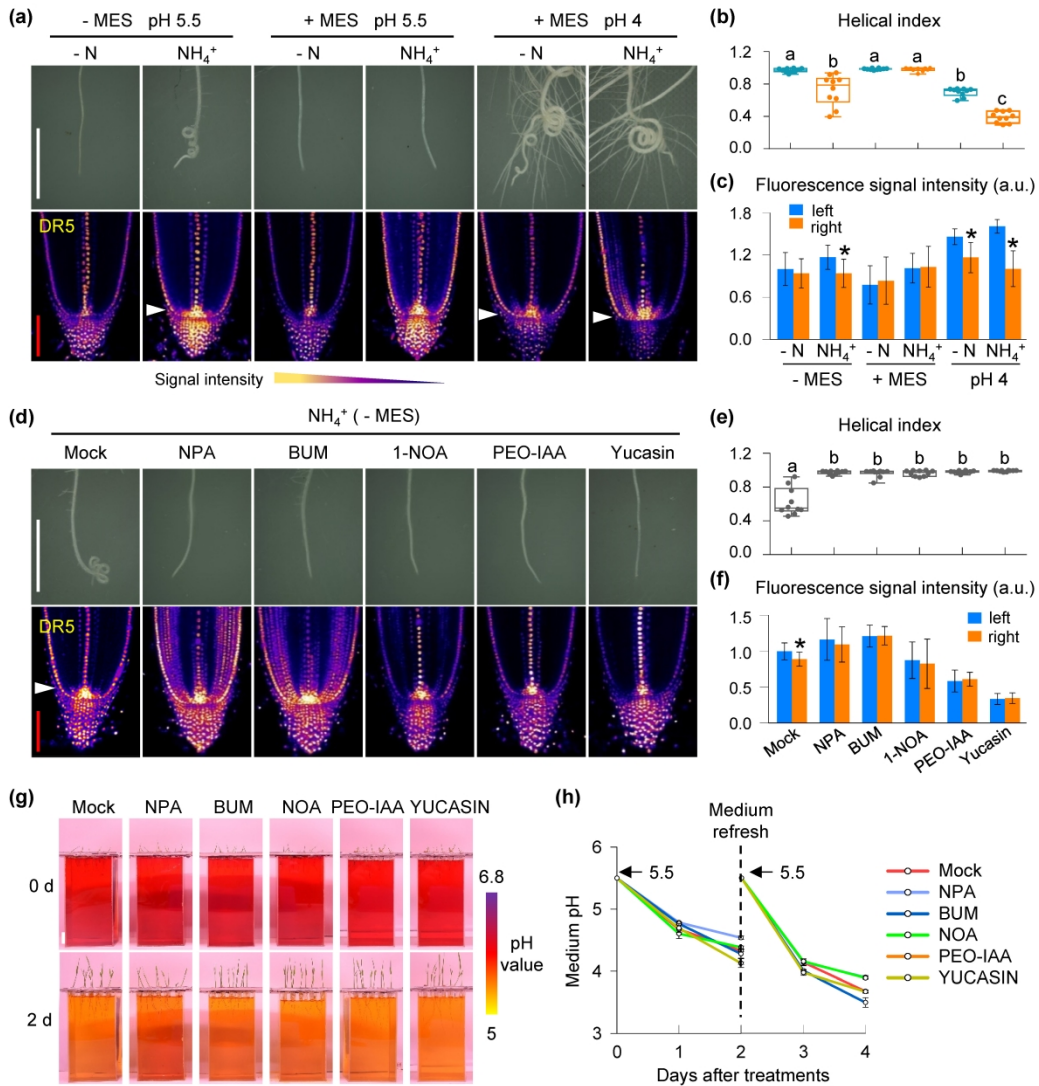
tpj_14978_f1.jpg



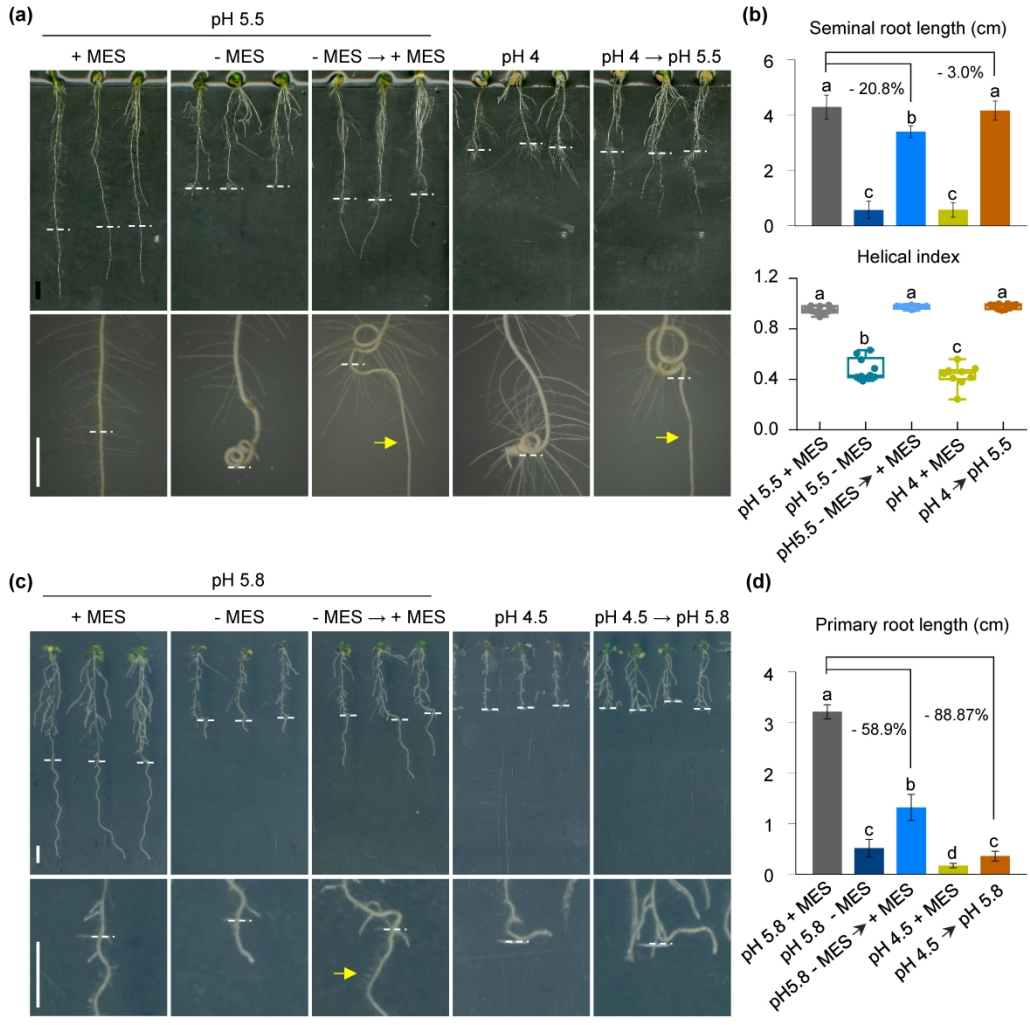
tpj_14978_f2.jpg



tpj_14978_f3.jpg



tpj_14978_f4.jpg



tpj_14978_f5.jpg